Supplementary Material (ESI) for Chemical Communications

Improved oxygen mobility in nanosized mixed-oxide particles synthesized using a simple nanocasting route

Magali Bonne, Nicolas Bion, Frédéric Pailloux, Sabine Valange, Sébastien Royer*, Jean-Michel Tatibouët and Daniel Duprez

Supporting information

Synthesis of the HMS support

To a solution containing 7.21 g of dodecylamine in 66 mL of absolute ethanol, 76 mL of water is added under stirring. After 90 min to ensure a complete homogeneity of the solution, 26.8 g of TEOS is slowly added to the solution containing the templating agent under vigorous stirring. After 30 min, stirring was slowed down and the mixture maintained under agitation for 18 h. After ageing, the white solid was recovered by filtration and washing with water. Finally the obtained white solid was dried at 75 °C for 2 days before being calcined under flowing air at 600 °C (temperature increase ramp = 1 °C min^{-1}, isothermal time = 6 hr).

Synthesis of the perovskite-based samples

The mass fraction of perovskite in the composite (perovskite on silica support) is fixed at 15 wt% (and 25 wt% for $LaFeO_3$), leading to the following samples 15LaFe(or 25LaFe)-HMS, 15LaCo-HMS and 15LaMn-HMS (Table 1). Corresponding masses of nitrate precursors ($La(NO_3)_3.6H_2O$ and $Co(NO_3)_2.6H_2O$ for $LaCoO_3$) are dissolved in distilled water, and glycine added as complexing agent (ratio $(NO_3)^-$/glycine = 1). The solution is then mixed with the HMS support, water evaporated, and temperature increased up to 280 °C for glycine auto-ignition (CAUTION: reaction is strongly exothermic and hot matter projection occurs during reaction). Before characterization, solids were calcined at 600 °C for 2 h. LaCo and LaMn reference bulk samples are prepared for comparison using similar self-combustion conditions ($(NO_3)^-$/glycine ratio fixed to 1).

Isotopic exchange reaction: theory and data treatment

The exchange mechanism can be described by the following equation, even if three different mechanisms are depicted:

$$^{18}O_g + {}^{16}O_s \Leftrightarrow {}^{16}O_g + {}^{18}O_s \quad (1)$$

The three mechanisms are:

Equilibration

This mechanism results from the adsorption/desorption process of an O_2 molecule from the gas phase on the surface of the oxide. This reaction does not require the participation of any oxygen ion from the oxide. Consequently, ^{18}O and ^{16}O fractions in the gas phase remains constant during the test. This reaction can be written as follows:

$$^{16}O_{2(g)} + {}^{18}O_{2(g)} \Leftrightarrow 2.\ {}^{18}O^{16}O_{(g)} \quad (2)$$

Simple heteroexchange

This exchange occurs with the participation of one oxygen ion from the structure of the solid. The two following equations characterize this mechanism:

$$^{18}O^{18}O_{(g)} + {}^{16}O_{(s)} \Leftrightarrow {}^{18}O^{16}O_{(g)} + {}^{18}O_{(s)} \quad (3)$$

$$^{18}O^{16}O_{(g)} + {}^{16}O_{(s)} \Leftrightarrow {}^{16}O^{16}O_{(g)} + {}^{18}O_{(s)} \quad (4)$$

Because of the reaction order to oxygen is close to 1 for the oxides presenting this mechanism as main mechanism, some authors supposed the formation of triatomic species (O_3^-) on the surface (Eley-Riedel mechanism). The formation of a triatomic complex with the two atoms originating from the gas phase and one atom of the surface atomic layer, is likely to occur because an oxygen dissociative mechanism on the surface would present a reaction order to oxygen close to 0.5.

Complex heteroexchange

In opposition to the simple heteroexchange, this mechanism is supposed to involve the participation of two atoms of the solid at each step:

$$^{18}O^{18}O_{(g)} + 2.^{16}O_{(s)} \Leftrightarrow {}^{16}O^{16}O_{(g)} + 2.^{18}O_{(s)} \quad (5)$$

And in the case of the occurrence of $^{16}O^{16}O$ isotopes in the gas phase:

$$^{18}O^{16}O_{(g)} + 2.^{16}O_{(s)} \Leftrightarrow {}^{16}O^{16}O_{(g)} + {}^{18}O_{(s)} + {}^{16}O_{(s)} \quad (6)$$

$$^{18}O^{16}O_{(g)} + 2.^{18}O_{(s)} \Leftrightarrow {}^{18}O^{18}O_{(g)} + {}^{18}O_{(s)} + {}^{16}O_{(s)} \quad (7)$$

An oxygen reaction order near 0.5 is observed for the oxides mainly exhibiting this mechanism (Cr_2O_3, V_2O_5, α-Fe_2O_3, NiO,…), that supposed a dissociative adsorption on the anionic vacancies on the surface of the solid. The formation of a quadriatomic intermediate was also considered by some authors. A "place exchange" mechanism, which consists only in the displacement of a preadsorbed O_2 molecule, and which does not require any O-O bond scission, was also proposed as a possible mechanism. In the scope of an extended research in superoxides (O_2^-) reactivity conducted in our laboratory and concerning the study of $Ce_xZr_{1-x}O_2$ surface by use of isotopic exchange followed by FTIR, we have reported that $^{16}O_2^-$ superoxides exchanged in one step to give selectively $^{18}O_2^-$. This corresponds well to a place exchange mechanism.

Data treatment

The rate of exchange (V_{ex}, $at.g^{-1}.min^{-1}$) is calculated from the rate of disappearance of ^{18}O from the phase gas at time t:

$$V_{ex} = -2.N_g.\frac{d\alpha_g{}^t}{dt} = 2.N_s.\frac{d\alpha_s{}^t}{dt} \quad (8)$$

with: N_g and N_s, total number of oxygen atoms in the gas phase and exchangeable at the surface of the solid
$\alpha_g{}^t$ and $\alpha_s{}^t$, ^{18}O atomic fraction in the gas phase and at the surface at each time

$\alpha_g{}^t$ is calculated from the partial pressure of $^{18}O_2$, $^{16}O_2$ and $^{16}O^{18}O$ at each time:

$$\alpha_g{}^t = \frac{\frac{1}{2}.P_{34}{}^t + P_{36}{}^t}{P_{32}{}^t + P_{34}{}^t + P_{36}{}^t} \quad (9)$$

and N_g is obtained from equation (10):

$$N_g = \frac{N_A.P_T}{R}.\left(\frac{V_r}{T_r} + \frac{V_c}{T_c}\right) \quad (10)$$

with: N_A, Avogadro number
P_T, total pressure
R, gas constant
V_r and V_c, volume of the heated and non heated part of the system
T_r and T_c, temperature of the heated and non heated part of the system

Then, the **number of exchanged atoms at 60 min** ($\mathbf{N_{ex}^{60}}$, Table 1) is calculated from the number of ^{18}O atoms at 60 min:

$$N_e{}^t = \left(\alpha_g{}^0 - \alpha_g{}^t\right)N_g \quad (11)$$

In the test conditions, the **initial rate of exchange** ($\mathbf{V^0_{ex}}$, Table 1) was calculated from the initial slopes (first 30 seconds) of $^{18}O_2$ ($\frac{dP_{36}{}^0}{dt}$) and $^{16}O^{18}O$ ($\frac{dP_{34}{}^0}{dt}$) with respect to time.

$$V_{ex} = -\frac{N_A}{R}.\left(\frac{V_r}{T_r} + \frac{V_c}{T_c}\right)\left(2.\frac{dP_{36}{}^0}{dt} + \frac{dP_{34}{}^0}{dt}\right) \quad (12)$$

The first order kinetic equation proposed by Boreskov (G. K. Boreskov, *Adv. Catal.* 1964, **15**, 285) was used to evaluate the **constant rate** ($\mathbf{K_{ex}}$, Table 1). Experimental exchange curves were fitted for t between 10 and 60 min in order to avoid carbonate contribution to the calculated constant rate value:

$$-Ln(\Gamma) = K\left(\frac{\lambda + 1}{N_g}\right)t \quad (13)$$

with: $$\Gamma = \frac{\alpha_g{}^t - \alpha^*}{\alpha_g{}^0 - \alpha^*}$$

$$\lambda = \frac{N_g}{N_s}$$

For the exchange experiment, 20 mg of catalyst was weighed and inserted in a microreactor between two quartz wool plugs. Then the sample was heated at its calcination temperature under O_2 (ramp = 10 K min^{-1} − D_{O2} = 20 mL min^{-1}). Thereafter, the sample was cooled to room temperature under O_2 and then heated again under dynamic vacuum until the temperature of the test was reached (ramp = 10 K min^{-1}). Pure $^{18}O_2$ at a pressure of about 56.0 mbar was introduced into the reactor. The partial pressure evolution of $^{18}O_2$ (mass 36), $^{16}O_2$ (mass 32), and $^{16}O^{18}O$ (mass 34) was followed on the mass spectrometer for an experiment time of 60 min. N_2 (mass 28) was also recorded to detect any possible leak.

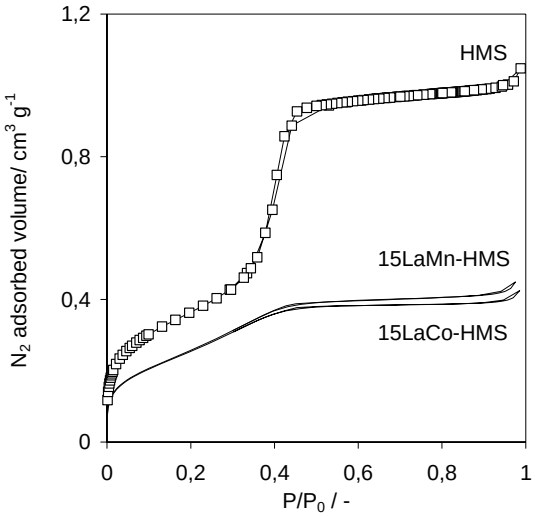

Fig. S1 N_2 adsorption/desorption isotherms at -196 °C obtained on HMS mesoporous silica support and on $LaCoO_3$ and $LaMnO_3$ supported perovskites.

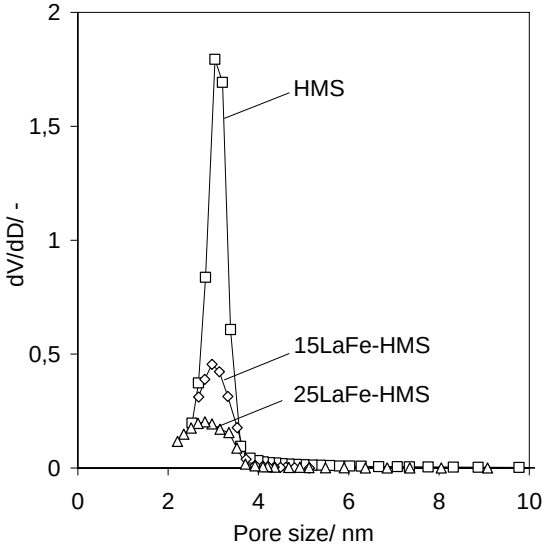

Fig. S2 BJH pore size distributions (desorption branch) on pure HMS silica and two supported $LaFeO_3$/HMS samples.

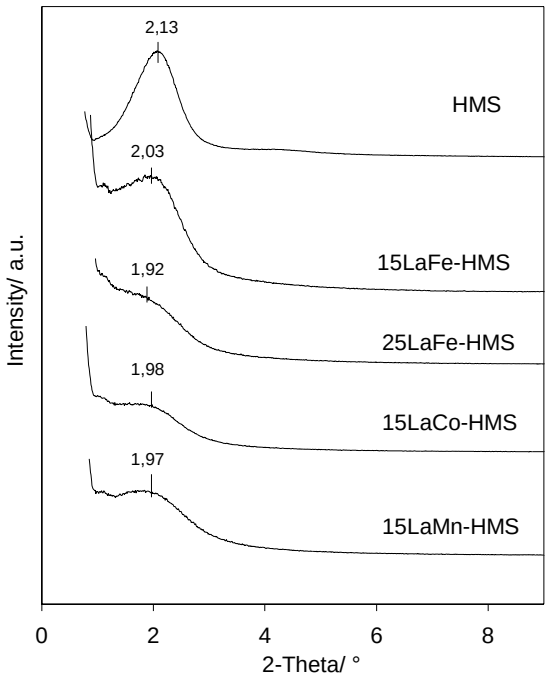

Fig. S3 Small angle X-ray diffraction patterns obtained for the two $LaFeO_3$/HMS samples compared with the parent HMS solid.

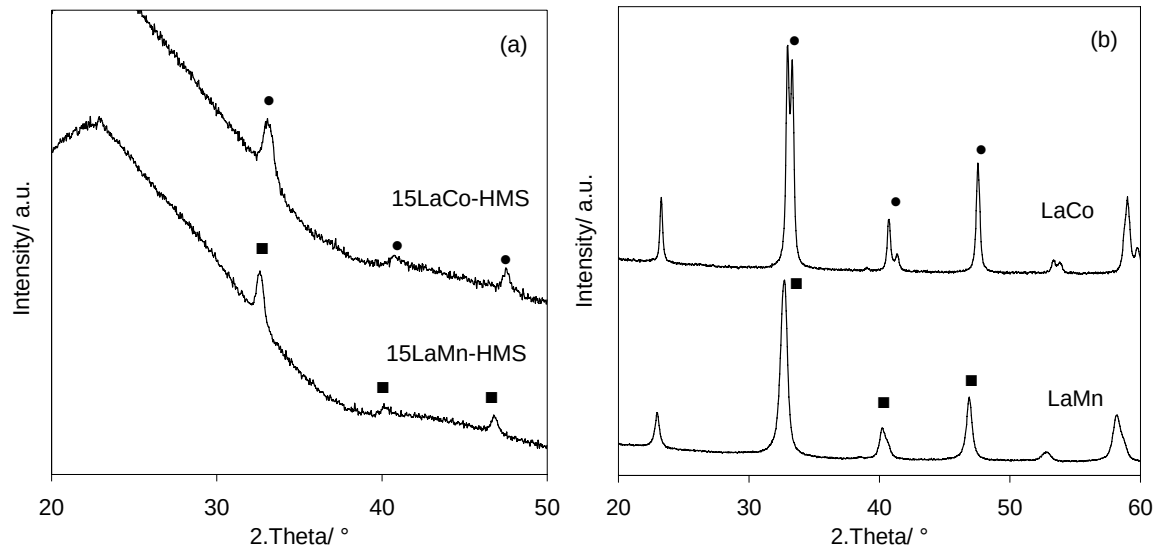

Fig. S4 X-ray diffraction patterns for: (a) 15LaCo-HMS and 15LaMn-HMS; (b) LaCo and LaMn reference bulk samples. Square: main characteristic peaks attributed to the rhombohedral $LaMnO_{3.15}$ structure (JCPDS file n°050-0298); Circle: main characteristic peaks attributed to the rhombohedral $LaFeO_3$ structure (JCPDS file n° 009-0358).

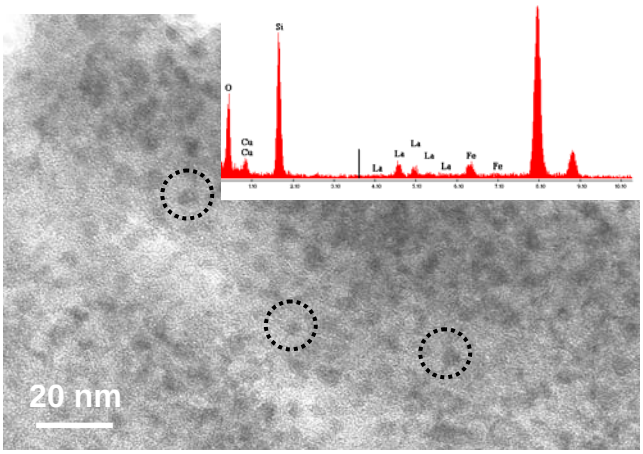

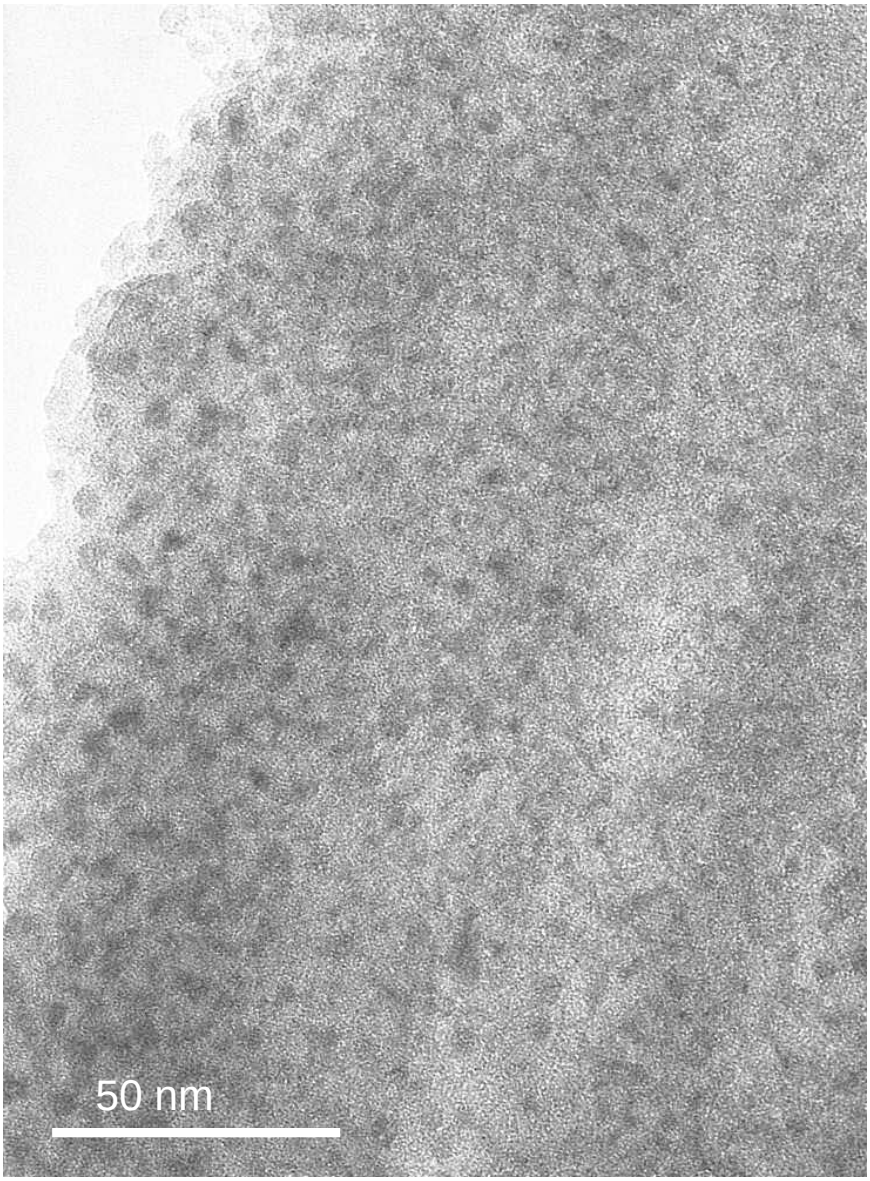

Fig. S5 Typical Transmission electron micrograph obtained for 20LaFe-HMS. Corresponding EDXS spectrum (inset).

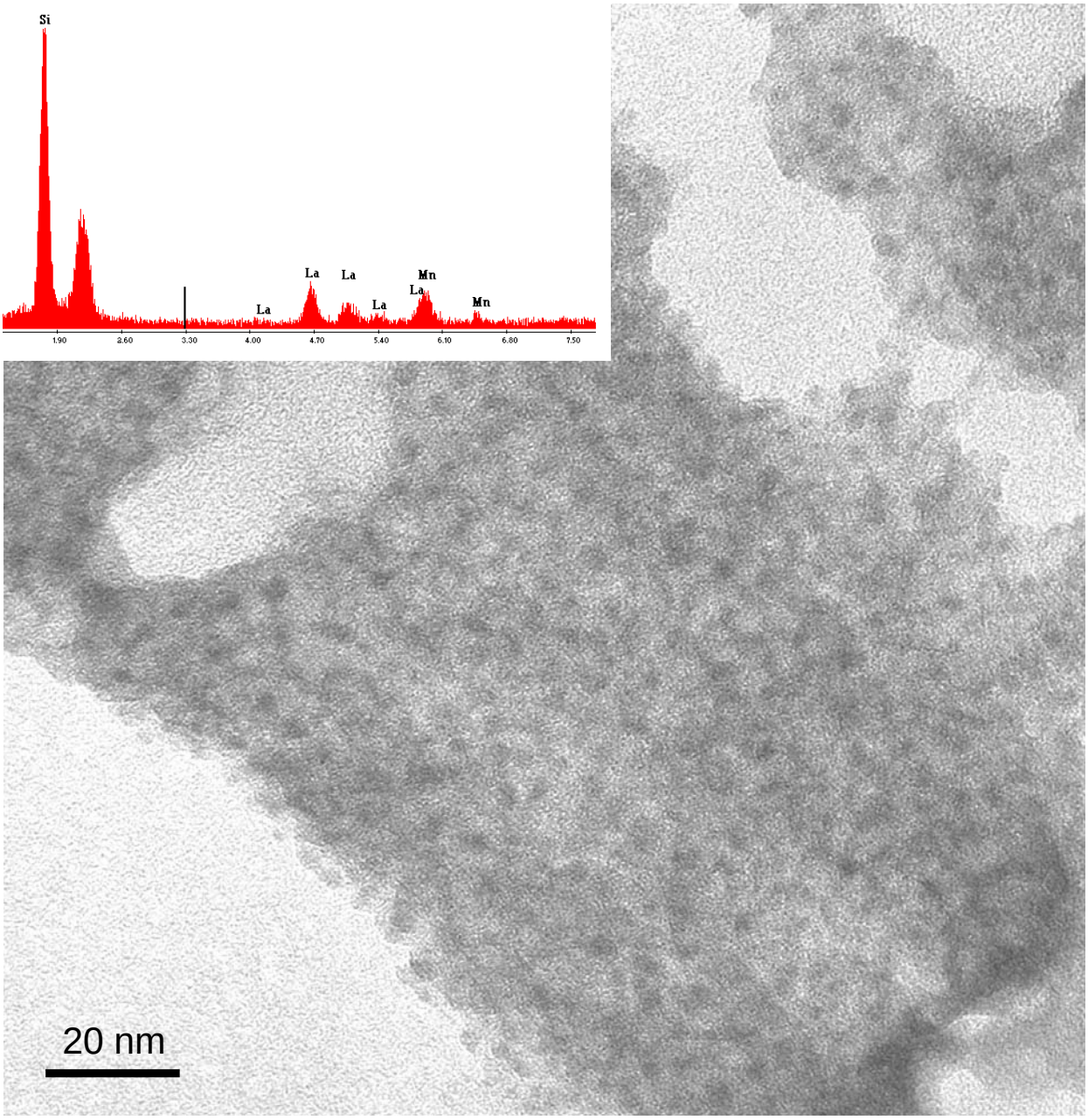

Fig. S6 Typical transmission electron micrograph and corresponding EDXS spectrum for 15LaMn-HMS. Nanometric particles are shown to be located all over the silica grain. As for the LaFe-based samples, no large external crystallized particles can be evidenced by TEM.

.

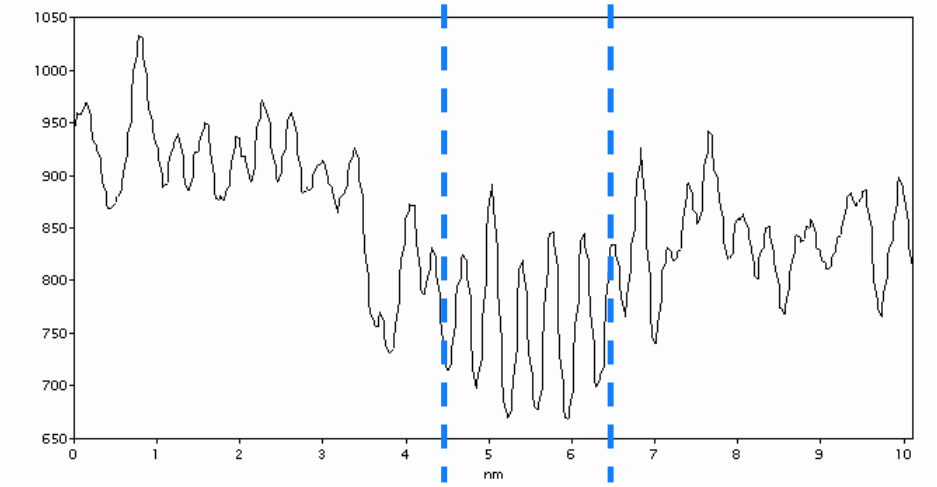

Fig. S7 Intensity profile of the particle presented Figure 2 (inset). A change in oscillation amplitude is observed between the two vertical dotted lines. This variation is due to the lattice fringes of the particle presented Figure 2(inset). The vertical dotted lines evidenced then the edge of the particle (about 2 nm).

.

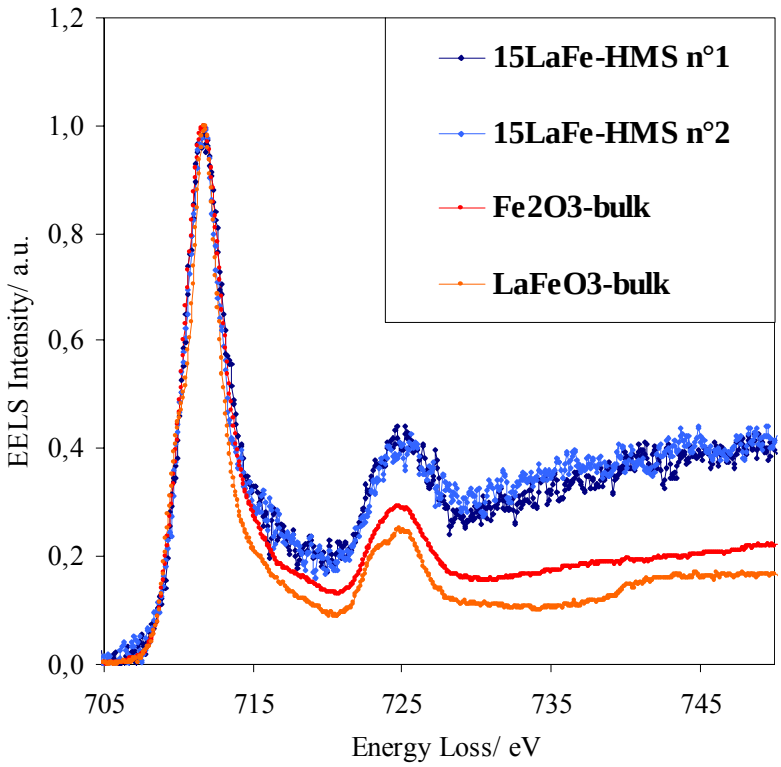

Fig. S8 EELS spectra of the Fe-$L_{2,3}$ edges obtained for the 15LaFe-HMS sample and comparison with bulk $LaFeO_3$ and Fe_2O_3 samples prepared according similar procedure. Before EELS spectroscopy, XRD was used to check the phase purity of the samples.

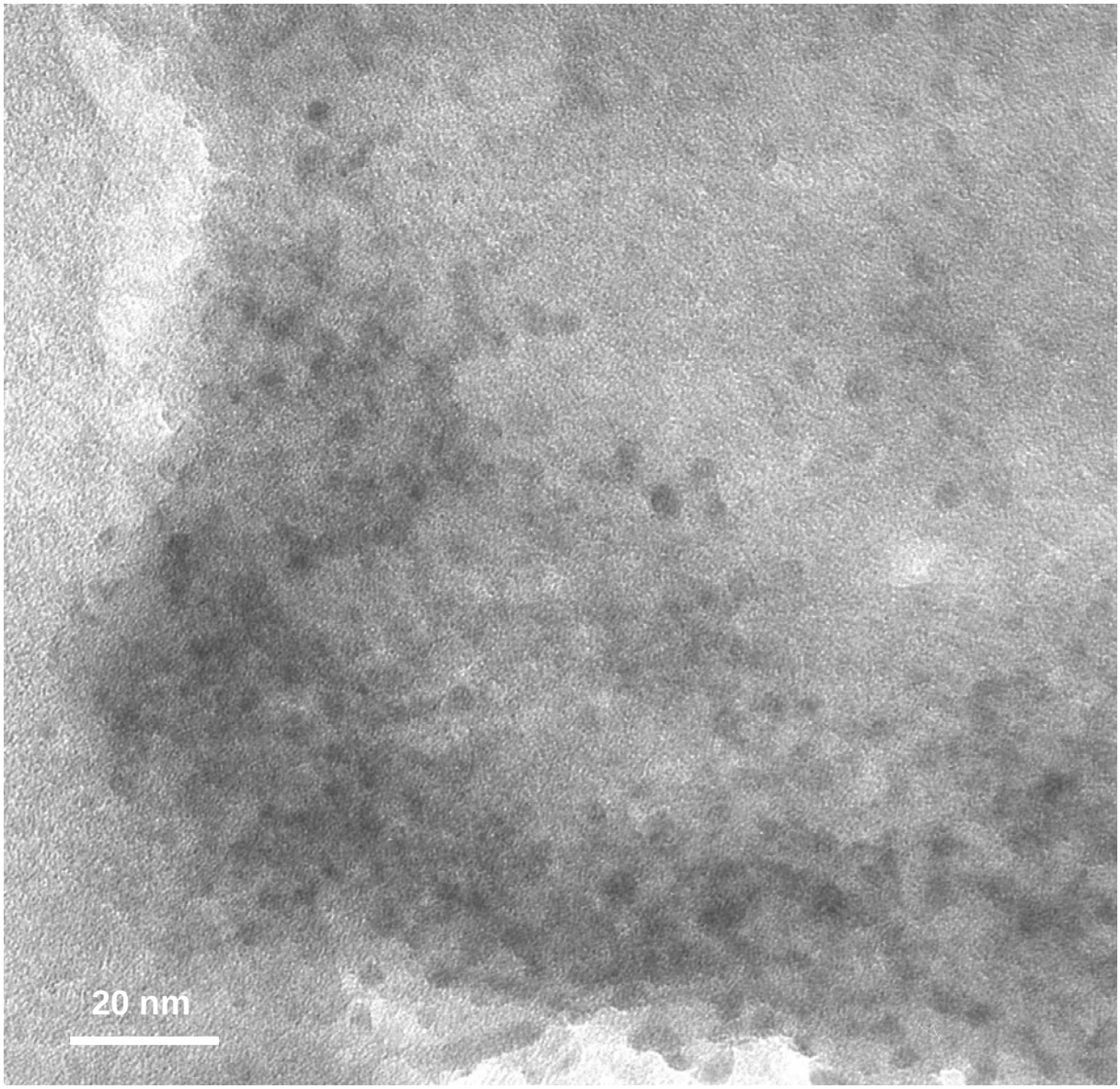

Fig. S9 Typical transmission electron micrograph for 15LaCo-HMS. Nanometric particles are shown to be located at the periphery of the silica grain, and only a few particles can be observed in the middle of the silica grain. As for the other samples, no large external crystallized particles can be evidenced by TEM.

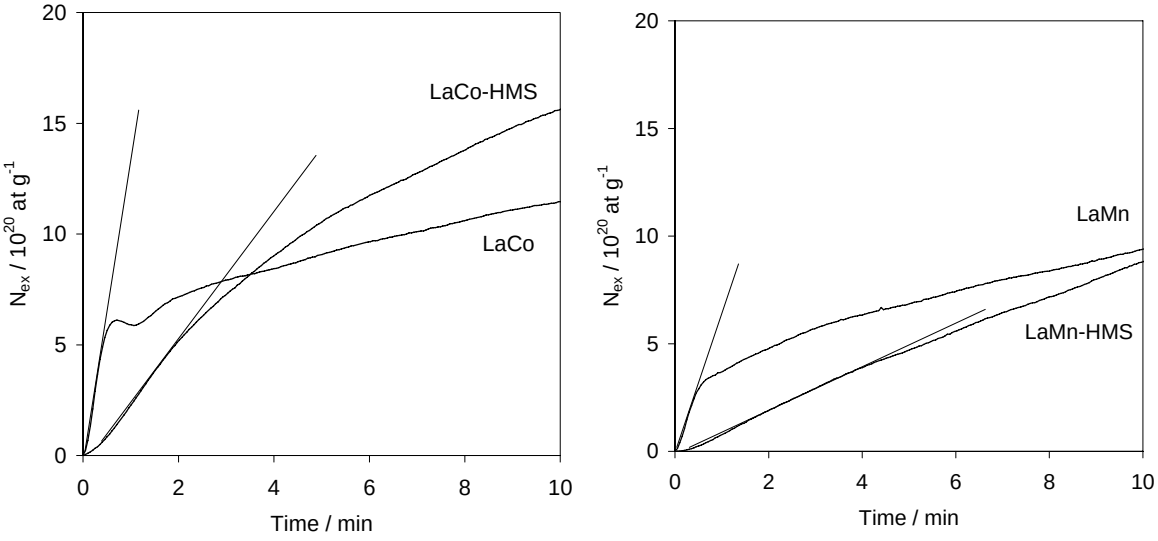

Fig. S10 Number of oxygen atoms exchanged (N_{ex}) versus time of reaction obtained at the beginning of exchange reaction (exchange experiment performed at T = 450 °C for 60 min). Tangent at t = 0 min: initial rate of exchange, values summarized in Table 1.

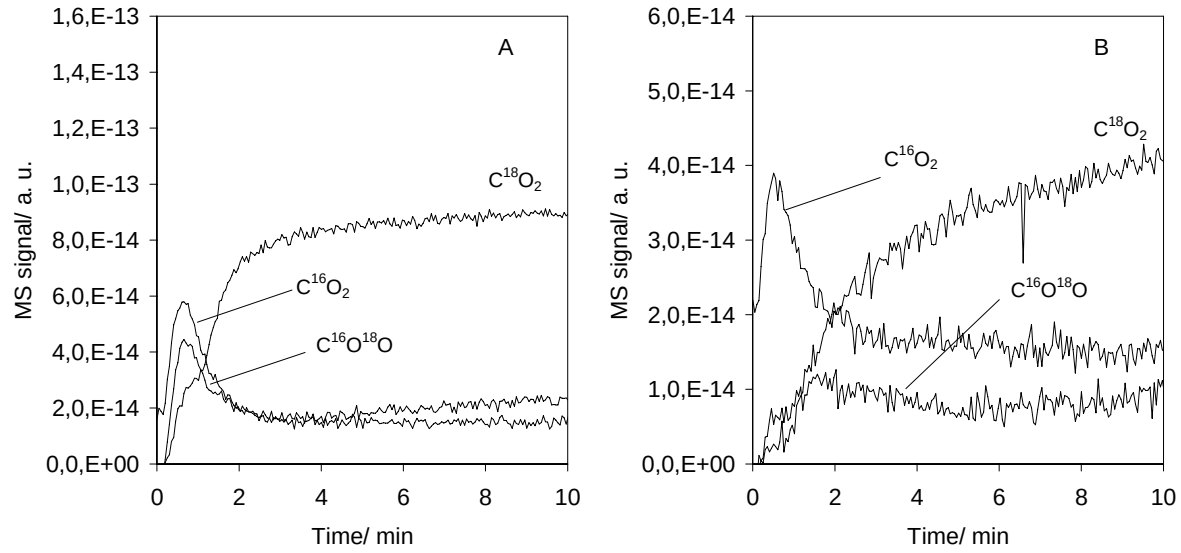

Fig. S11 Evolution of the $C^{18}O^{16}O$ mass spectrometer signal obtained over bulk LaCo (A) and LaMn (B) reference solids.

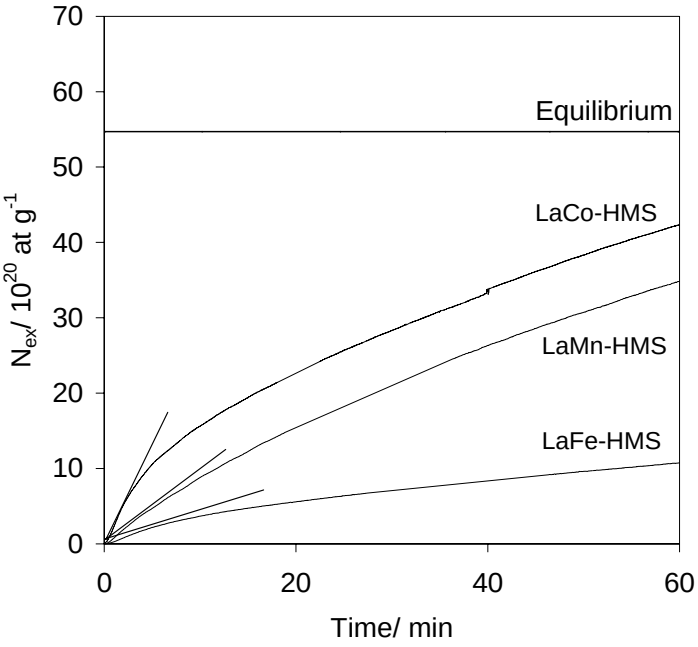

Fig. S12 Number of oxygen atoms exchanged (N_{ex}) versus time of reaction obtained for the three HMS supported samples. Exchange at T = 450 °C for 60 min. Equilibrium: calculated assuming equal fractions of ^{18}O in gas phase and bulk solid. Tangents at t = 0 min: initial rate of exchange. LaCo-HMS and LaMn-HMS exhibited high initial rate of exchange and high oxygen exchange capacity, while a far lower activity is obtained for the LaFe-HMS sample (Table 1 and Fig. S12). The activity order in oxygen exchange is in accordance with that reported by several authors over bulk perovskite of similar compositions for hydrocarbon oxidation reactions.[14] The differences in exchange activity observed between the supported samples is then mainly related to the activity of the B- element (Co, Mn or Fe).